min at maximal power output. The opalescent emulsion was centrifuged for 20 min at 20,000*g* to remove aggregated material. Fluorescence resonance energy transfer assays were performed as described (*10*). In Fig. 2, A and B, 40 μg of purified synaptotagmin or synaptophysin were incubated with 10 μg of liposomes in 1 ml of 20 mM tris-Cl (pH 7.2), 100 mM NaCl, 0.5 mM EGTA. The free Ca^{2+} concentration was increased by successive additions of 20 mM or 100 mM solutions of $CaCl_2$ to give the free Ca^{2+} concentrations indicated. In Fig. 2C, synaptotagmin was purified from a membrane extract prepared in 1% sodium cholate instead of Triton X-100, dialyzed against 20 mM tris-Cl (pH 7.2), 100 mM NaCl, 1% sodium cholate, 2 mM phenylmethylsulfonyl fluoride, and Pepstatin A (1 μg/ml) and combined with 60 μg of phospholipids per 100 μg of synaptotagmin resuspended in the same buffer (10% phosphatidylserine, 45% phosphatidylcholine, 45% phosphatidylethanolamine). Liposomes were formed by dialysis against cholate-free buffer.

14. In all proteolysis experiments, the degree of proteolysis was monitored by SDS-PAGE, followed by fragment visualization with site-specific antibodies (*3*). Conditions were chosen in which all synaptotagmin was cleaved but only minor further degradation of the fragments had occurred.
15. In the sucrose gradient centrifugations crude synaptic vesicles were solubilized with 1% (w/v) SDS or 2% (w/v) CHAPS, cholate, or β-octylglucoside in 75 mM tris-Cl (pH 7.4), 1 mM EDTA. Solubilized proteins were loaded on 11.8 ml of 5 to 20% (w/v) sucrose gradients containing 0.1% of the respective detergent in the same buffer as above. For SDS-solubilized proteins, 350 μg of total protein were loaded in a 100-μl volume; for all other detergents, 260 μg of total protein were loaded in a 300-μl volume. Gradients were centrifuged for 16 hours at 4°C at 38,000 rpm in a Beckman SW41 rotor and fractionated into 24 0.5-ml fractions. For the experiments utilizing partially trypsinized synaptotagmin, synaptic vesicles were incubated with trypsin in a protein mass ratio of 1:6000 before solubilization, and samples were solubilized in CHAPS or SDS. On parallel gradients, the positions of molecular size markers were as follows: carbonic anhydrase (29 kD), fractions 2 and 3; bovine serum albumin (67 kD), fraction 4; alcohol dehydrogenase (155 kD), fraction 6; β-amylase (200 kD), fraction 8; apoferritin (443 kD), fractions 14 and 15. We analyzed fractions by SDS-PAGE and immunoblotting, using the Amersham enhanced chemiluminescence system according to the manufacturer's directions with polyclonal antibodies to the NH_2-terminus and the C_2 domains of synaptotagmin as described (*3*).
16. We thank M. D. Bazzi for advice concerning the Ca^{2+} equilibrium dialysis and fluorescence resonance energy transfer experiments, H. Schauerte and S. Schieback for help in some of the experiments, and P. R. Maycox for critical reading of the manuscript.

23 December 1991; accepted 9 March 1992

High-Frequency Network Oscillation in the Hippocampus

György Buzsáki,* Zsolt Horváth, Ronald Urioste, Jamille Hetke, Kensall Wise

Pyramidal cells in the CA1 hippocampal region displayed transient network oscillations (200 hertz) during behavioral immobility, consummatory behaviors, and slow-wave sleep. Simultaneous, multisite recordings revealed temporal and spatial coherence of neuronal activity during population oscillations. Participating pyramidal cells discharged at a rate lower than the frequency of the population oscillation, and their action potentials were phase locked to the negative phase of the simultaneously recorded oscillatory field potentials. In contrast, interneurons discharged at population frequency during the field oscillations. Thus, synchronous output of cooperating CA1 pyramidal cells may serve to induce synaptic enhancement in target structures of the hippocampus.

Much of what is known about the physiological function of the hippocampus is based on in vivo and in vitro studies of sequentially analyzed single neurons (*1*, *2*). Although it has long been believed that the computational power of complex neuronal networks cannot be recognized by the properties of single cells alone (*3*), experimental access to the emergent properties of cooperating hippocampal neurons has been difficult. Direct investigation of the time-varying organization of neuronal populations requires the simultaneous observation of many individual neurons in the awake animal (*4*). Using silicon multichannel recording arrays (*5*), we report here the physiological details of a high-frequency oscillation of the hippocampal CA1 neuronal network that is a specific product of cellular cooperativity.

The data analyzed in this study were recorded from 19 adult male rats. Local field potentials and unit activity were recorded by multichannel microprobes (*5*, *6*) in the rat during spontaneous behaviors and sleep (*7*). The oscillatory behavior of the recorded cell populations and local field potentials was determined by the periodic modulation of the auto- and cross-correlograms (*8*).

Local field potentials in the CA1 strata pyramidale and radiatum were related to cellular firing during awake immobility (Fig. 1). Sharp waves in the stratum radiatum of the CA1 network reflect depolarization of the apical dendrites of pyramidal cells by the Schaffer collaterals, which is a result of the synchronous bursting of CA3 pyramidal cells (*9*, *10*). In conjunction with the stratum radiatum sharp waves, fast field oscillations were present in the CA1 pyramidal layer (*1*, *9*, *10*). The spindle-shaped oscillatory pattern consisted of 5 to 15 sinusoid waves with 200-Hz intraburst frequency. Neuronal discharges most often occurred during the local field oscillations. Isolated pyramidal cells usually fired a single action potential during the field oscillations but occasionally fired a burst of two to three spikes (*11*). The probability of spike bursts (complex spikes) was three to eight times higher during the fast field oscillations than during comparable time periods in their absence.

The laminar distribution of the fast field oscillations was determined by advancing linear arrays of electrodes (*6*) perpendicular to the CA1 pyramidal layer. Amplitude maxima of the fast field oscillations were found in the pyramidal layer (0.2 to 1 mV), and the polarity of the signal reversed in phase about 100 μm below the pyramidal layer, which suggests that the main current source of the extracellularly recorded fast field oscillations is the cell bodies of pyramidal cells.

Typically, less than 15% of the recorded neurons were active during a single oscillatory epoch. When discharges of all neurons

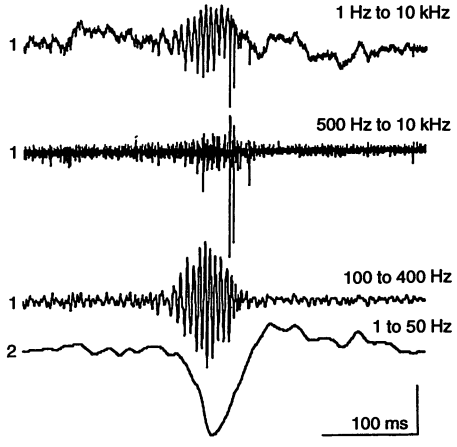

Fig. 1. Fast field oscillation in the CA1 region of the dorsal hippocampus. Simultaneous recordings from the CA1 pyramidal layer (electrode 1) and stratum radiatum (electrode 2). Uppermost trace of electrode 1 is wide-band recording (1 Hz to 10 kHz). Second and third traces are digitally filtered derivatives of the wide-band trace (unit activity 500 Hz to 10 kHz and fast field oscillation (100 to 400 Hz). Note simultaneous occurrence of fast field oscillations, unit discharges, and sharp wave (electrode 2). Electrode 2 was 200 μm below the pyramidal layer. Calibrations: 0.5 mV (trace 1), 0.25 mV (traces 2 and 3), and 1.0 mV (trace 4).

G. Buzsáki, Z. Horváth, R. Urioste, Center for Molecular and Behavioral Neuroscience, Rutgers University, 197 University Avenue, Newark, NJ 07102.
J. Hetke and K. Wise, Center for Integrated Sensors and Circuits, University of Michigan, Ann Arbor, MI 48109.

*To whom correspondence should be addressed.

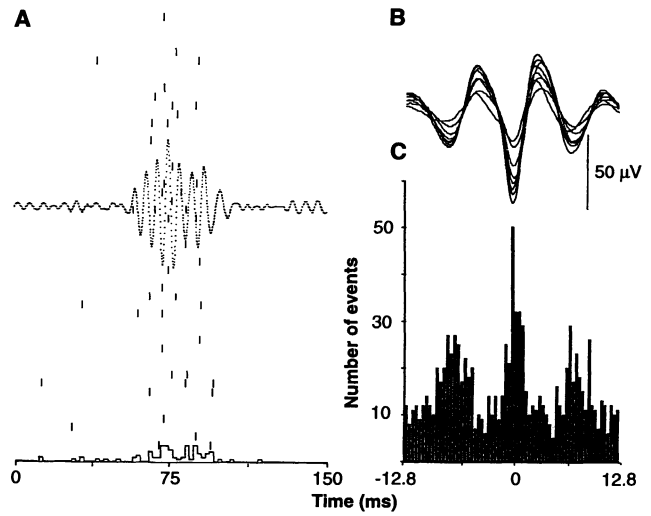

Fig. 2. High-frequency oscillation of the CA1 network. (**A**) Fast field oscillation–associated discharges of 50 simultaneously recorded pyramidal neurons with a 24-site probe. Trace is an average of simultaneously recorded field activity (100 to 400 Hz) from eight sites. Vertical lines are discriminated action potentials. Only 32 of the 50 units emitted action potentials during the trace. Histogram presents averaged momentary firing of pyramidal cells. (**B**) Superimposed averaged traces from eight different recording sites (maximum interelectrode distance was 1.8 mm). Averaged traces are virtually synchronized. (**C**) Cross-correlogram of all 50 units, with the negative peaks of fast field oscillatory waves as time zero. Time scale is as in (B). Neurons fire on the negative peaks of fast field oscillatory cycles.

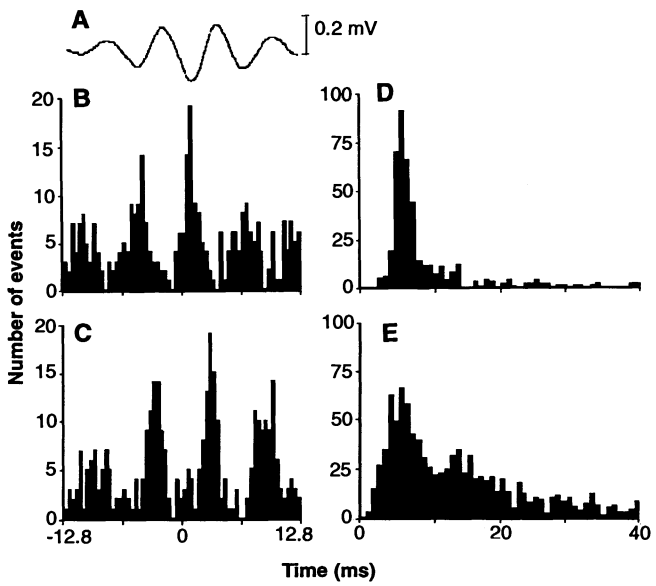

Fig. 3. Fast field oscillation–associated activity of local circuit neurons. (**A**) Average of 128 fast field oscillatory events. (**B**) Summed cross-correlogram of simultaneously recorded pyramidal cells (n = 21) from seven different sites. (**C**) Cross-correlogram of a single local circuit neuron (stratum oriens) simultaneously recorded with the pyramidal cells. The local circuit neuron discharged predominantly on the positive phase of the fast field oscillatory cycles. (**D**) Cycle duration histogram of fast field oscillation (n = 1024). (**E**) Interspike interval histogram of the local circuit interneuron.

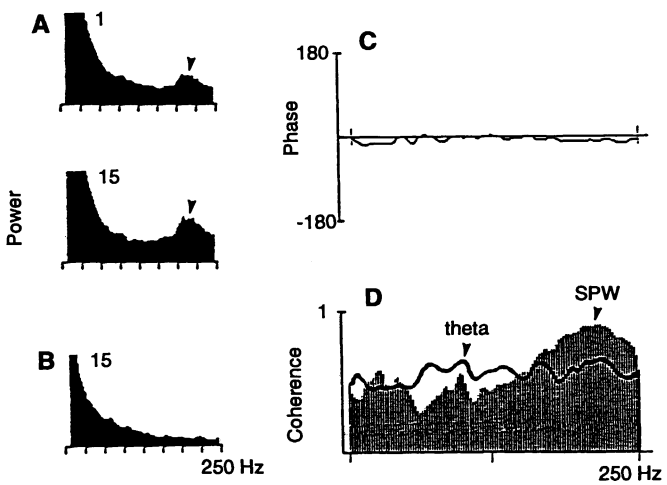

Fig. 4. Spatial coherence of the high-frequency oscillation. Power spectra of local field potentials during immobility (**A**) and during walking with theta activity (**B**). Electrodes 1 and 15 were in the CA1 pyramidal layer. Electrodes were separated by 1.2 mm. Power peaks are at approximately 200 Hz (arrows). Ordinate: linear scale; arbitrary units. (**C**) Phase plot of the local field potential pair during immobility. (**D**) Coherence plots of the local field potential pair during sharp wave–associated immobility (SPW) and theta behaviors.

were summed as a function of time, peaks of maximum neuronal activity often coincided with the negative peaks of the simultaneously recorded field oscillation (Fig. 2). Cross-correlograms (n > 500 from 18 rats) of several hundred epochs revealed that the probability of discharge of pyramidal cells was highest during the negative peaks of the oscillatory field potential. Similarly, cross-correlation of isolated unit pairs resulted in rhythmic peaks at the frequency of the oscillatory field potential (8 out of 12 pairs), even though the autocorrelation histograms of the spike trains never revealed peaks at the population frequency.

In contrast to pyramidal cells, seven of the ten physiologically identified interneurons in the strata oriens and pyramidale fired rhythmically at the fast population frequency (Fig. 3), and the peaks of the cross-correlograms were time-shifted by almost a half cycle relative to the peaks of the summed pyramidal cells. The frequency of firing of three interneurons (modal peaks: 50, 72, 140 spikes/s, respectively) was lower than the population firing frequency, but these interneurons also fired in phase with the population rhythm.

Spatial coherence of population synchrony was studied by evenly spaced multishank electrode arrays positioned along the longitudinal axis of the hippocampus. Simultaneously recorded traces were synchronous during the emergence of the field oscillation (Fig. 2B). Synchrony was established within one to two cycles. Similar establishment of oscillations without any phase lag was also observed at our maximum electrode spacing (2.2 mm), corresponding to approximately one-quarter of the length of the rat hippocampus.

Spatial cooperativity of CA1 cells during the fast field oscillatory potentials was further demonstrated by coherence spectral analysis (Fig. 4). Power spectra of epochs containing fast oscillatory patterns revealed peaks at 150 to 250 Hz. The electrode distance for these measurements varied from 0.4 to 2.2 mm along the longitudinal axis of the dorsal CA1 region.

Despite the synchronous emergence of fast oscillatory field potentials and associated sharp waves in the two hippocampi, cross-correlograms of field oscillations recorded from identical positions in the ipsi- and contralateral CA1 regions were flat. This result indicates the lack of interhemispheric phase locking of the oscillations.

Recordings from the CA3 pyramidal layer of five rats also revealed high-frequency oscillation in this region. However, the dominant frequency of the field oscillations was about 100 Hz, and simultaneously recorded sites did not show the high spatiotemporal coherence observed in the CA1 region. These findings, together with the lack of bilateral CA1 synchrony of the fast field cycles, suggest that fast oscillatory field potentials (200 Hz) are gen-

erated by the CA1 circuitry.

The high-frequency population oscillation (200 Hz) indicates precise temporal coherence of pyramidal cell firing. CA1 pyramidal neurons and interneurons are excited by the CA3 Schaffer collaterals during hippocampal sharp waves (9). We hypothesize that transient but powerful depolarization of the excited interneurons results in high-frequency firing of these cells which, in turn, determine the precise timing of pyramidal cell discharges. Inhibitory neurons may not cause the population oscillation but may control the timing of the action potentials of pyramidal cells in the background of an excitatory CA3 barrage. Feedforward and recurrent excitation of inhibitory cells, as well as specific membrane conductances in interneurons, are required for the generation of the population oscillation in the neocortex and may be operative in the CA1 region as well (*12*). When sufficiently activated, the CA1 network shifts into a fast, transient rhythmic activity, the frequency of which is determined by the time constants of the membrane conductances of the interneurons.

The remote populations of CA1 pyramidal cells with extremely sparse excitatory collaterals (*13*) became synchronized without a time lag. Spatial synchrony in this region may be brought about by interactive interneurons or by mutual effects of pyramidal cells (*14*). Fast entrainment of inhibitory interneurons at the observed frequency may be possible by mutual excitation (*15*) or by communication through interneuronal gap junctions (*16*). Synchronization of pyramidal cells in the absence of excitatory collaterals may be brought about by ephaptic effects (*17*). The voltage gradient across the pyramidal cell layer during the emergence of field oscillations will affect voltage-dependent transmembrane currents and increase coherent firing of pyramidal cells.

The coherent bursts of CA1 pyramidal cells can produce very large transient depolarizations on their postsynaptic targets in retrohippocampal areas. Transient postsynaptic depolarization is a prerequisite of long-term synaptic modification (*18*). Neuronal bursts associated with theta rhythm have been hypothesized to be a physiological candidate of long-term synaptic potentiation (*19*). The powerful synchrony of pyramidal cells during hippocampal sharp waves offers an alternative mechanism to theta-related bursting. We hypothesize that synaptic modification in hippocampal target structures is induced during population oscillatory activity of the CA1 pyramidal cells.

REFERENCES AND NOTES

1. J. O'Keefe and L. Nadel, *The Hippocampus as a Cognitive Map* (Clarendon, Oxford, 1978).
2. M. Baudry and J. L. Davis, Eds., *Long-Term Potentiation: A Debate of Current Issues* (MIT Press, Cambridge, MA, 1991).
3. G. Gerstein, D. H. Perkel, J. Dayhoff, *J. Neurosci.* **5**, 881 (1985); R. D. Traub, R. Miles, R. K. S. Wong, *Science* **243**, 1319 (1989); T. J. Sejnowski, C. Koch, P. S. Churchland, *ibid.* **241**, 1299 (1988).
4. G. J. Krüger and J. D. Becker, *Trends Neurosci.* **7**, 1001 (1991).
5. K. D. Wise and K. Najafi, *Science* **254**, 1335 (1991).
6. The rats were anesthetized with ketamine-xylazine. Four types of movable recording electrodes were chronically implanted [G. Buzsáki *et al.*, *J. Neurosci. Methods* **28**, 209 (1989)]: (i) tungsten microelectrodes (1- to 5-μm tips), (ii) arrays of eight tungsten microelectrodes separated by 300 μm, (iii) single shank silicon probes (15 μm thick by 30 μm wide) with five recording sites (5 by 15 μm each) and 100-μm recording site separation, and (iv) "comb" silicon electrodes with 24 recording sites. The vertical four recording sites (6 by 6 μm) were spaced 50 μm apart and the six shanks (100 μm wide at the base, narrowing to 15 μm at the tip) were 300 μm apart. In addition, two to four microwires (60 μm) were inserted into the left hippocampus with tips in the strata pyramidale or radiatum of CA1. A pair of stimulating electrodes was implanted into the right angular bundle.
7. Local field potentials and unit activity were recorded (wide band: 3 Hz to 8 kHz) on optical disks. We recorded up to 16 channels of data simultaneously, using a 10-kHz sampling rate on each channel and 12-bit resolution.
8. A K-means clustering algorithm was used for spike separation. The spikes were represented as points in a ten-dimensional feature-space, and the dissimilarity of their shapes was measured as the Euclidean distance between the corresponding points in that space. An iterative procedure was used to find the local minimum of the partition error, and the number of separate unit clusters was determined by variance ratios [D. H. Perkel, G. L. Gerstein, G. M. Moore, *Biophys. J.* **7**, 327 (1967)]. The negative peaks of the fast field oscillations were detected, and the resulting pulses served as reference signals for the construction of cross-correlograms. Power spectra, phase spectra, and coherence spectra were computed between 3 and 250 Hz.
9. G. Buzsáki, L. Leung, C. H. Vanderwolf, *Brain Res. Rev.* **6**, 139 (1983), G. Buzsáki, *Brain Res.* **398**, 242 (1986), *Neuroscience* **31**, 551 (1989).
10. S. S. Suzuki and G. K. Smith, *Electroencephal. Clin. Neurophysiol.* **67**, 438 (1987).
11. Bursts of spikes with decreasing amplitude (complex spikes) unequivocally identify pyramidal cells in the CA1 region [S. E. Fox and J. B. Ranck, Jr., *Exp. Brain Res.* **41**, 299 (1981), G. Buzsáki and E. Eidelberg, *J. Neurophysiol.* **48**, 597 (1982)] Interneurons responded with repetitive discharges to stimulation, and their spontaneous activity was always faster than 10 Hz.
12. R. R. Llinás, *Science* **242**, 1654 (1988). J. Lacaille and S. Williams, *Neuroscience* **36**, 349 (1990); W. W. Lytton and T. J. Sejnowski, *J. Neurophysiol.* **66**, 1059 (1991); P. C. Bush and R. J. Douglas, *Neural Comput.* **3**, 19 (1991).
13. E. P. Christian and F. E. Dudek, *J. Neurophysiol.* **59**, 110 (1988), D. M. Finch, N. L. Nowlin, T. L. Babb, *Brain Res.* **271**, 201 (1983), N. Tamamaki, K. Abe, Y. Nojyo, *Brain Res.* **452**, 255 (1988).
14. M. Kuperstein, H. Eichenbaum, T. VanDeMark, *Exp. Brain Res.* **61**, 438 (1986).
15. H. B. Michelson and R. K. S. Wong, *Science* **253**, 1420 (1991).
16. H. Katsumaru, T. Kosaka, C. W. Heizman, K. Hama, *Exp. Brain Res.* **72**, 363 (1988).
17. R. Traub, E. Dudek, R. W. Snow, W. D. Knowles, *Neuroscience* **15**, 947 (1985); J. G. R. Jefferys and H. L. Haas, *Nature* **300**, 448 (1982), C. P. Taylor and F. E. Dudek, *Science* **218**, 810 (1982).
18. G. L. Collingridge, S. J. Kehl, H. McLennan, *J. Physiol.* **334**, 33 (1983); T. V. P. Bliss and T. Lomo, *ibid.* **232**, 331 (1973).
19. J. Larson and G. Lynch, *Science* **232**, 985 (1986); G. M. Rose and T. V. Dunviddie, *Neurosci. Lett.* **69**, 244 (1986), C. Pavlides, Y. J. Greenstein, M. Grudman, J. Winson, *Brain Res.* **439**, 383 (1988), T Otto, H. Eichenbaum, S. I. Wiener, C. G. Wible, *Hippocampus* **1**, 181 (1991).

20. Supported by the National Institutes of Health (grants NS27058 and 02383), the Human Frontier Science Program, and the Whitehall Foundation. We thank J. B. Ranck, Jr., T. J. Sejnowski, R. D. Traub, D. W. Tank, and R. K. S. Wong for helpful discussions.

17 January 1992, accepted 26 March 1992

Acquisition of Myogenic Specificity by Replacement of Three Amino Acid Residues from MyoD into E12

Robert L. Davis and Harold Weintraub*

The basic helix-loop-helix (bHLH) protein MyoD is a transcription factor that is important for the induction of the myogenic phenotype. The DNA binding basic region (13 amino acids) is necessary for recognition of the consensus MyoD binding site, for transcriptional activation, and for conversion of fibroblasts to muscle. In contrast, the non-tissue–specific bHLH protein E12 can bind to the MyoD binding site but does not induce myogenesis. Here, it is shown that only two amino acids in the MyoD basic region and a single amino acid from the junction, which separates the basic region and helix 1, are sufficient for myogenic specificity when substituted into the corresponding region of E12. These findings suggest that the recognition of particular determinants in the basic region is required for conversion of fibroblasts to muscle.

Expression of MyoD in a large number of cell types leads to their conversion to muscle (*1*). Only 68 amino acids of MyoD, consisting of the bHLH domain, are necessary and sufficient for myogenic conversion of stably transfected 10T½ fibroblasts (*2*). MyoD is a muscle-specific transcription factor that binds to most muscle-specific enhancer sequences, through specific CANNTG motifs (N = specific subsets of nucleotides), to activate muscle-specific gene expression (*3*).

Howard Hughes Medical Institute Laboratory, Fred Hutchinson Cancer Research Center, Seattle, WA 98104.

*To whom correspondence should be addressed.